



Effects of different long-term cropping systems on phosphorus adsorption and desorption characteristics in red soils

Xiaomei Gou¹ · Yan Cai¹ · Changquan Wang¹ · Bing Li¹ · Yi Zhang¹ · Xiaoyan Tang¹ · Jie Shen¹ · Zehui Cai¹

Received: 21 June 2019 / Accepted: 2 October 2019 / Published online: 22 November 2019
© Springer-Verlag GmbH Germany, part of Springer Nature 2019

Abstract

Purpose Phosphorus (P) fertilizer has been applied in regions with red soils to ensure high crop yield. However, the supply of bioavailable P for crop plants is insufficient due to the strong adsorption and fixing behaviors in red soils. In this study, we explored P adsorption and desorption characteristics in red soils under different long-term cropping systems. We also analyzed how the cropping systems affect P adsorption and desorption through changing soil physicochemical properties under the experimental conditions.

Materials and methods Eighteen red soil samples were collected at depths of 0–20 cm from six cropping systems (abandoned farmland, corn continuous cropping, taro continuous cropping, pea–corn rotation, canola–tobacco rotation, and walnut–tobacco intercropping for at least 10 years) in Miyi County, Sichuan Province, China. Soil physicochemical properties, zeta potentials, and P adsorption and desorption characteristics were evaluated.

Results and discussion The P adsorption capacity of soils increased at a decreasing rate with increasing exogenous P concentration, while the P desorption capacity increased constantly; however, the change in the percentage of desorbed P had no clear trend. The soils under pea–corn rotation and taro continuous cropping had lower P adsorption capacities and higher P desorption capacities compared to those under the other cropping systems. The maximum P adsorption capacities (Q_m) of pea–corn rotation and taro continuous cropping soils were 16.1% and 32.4% of abandoned farmland soil, while the corresponding desorption coefficients were 6.93 and 1.62 times higher than that of abandoned farmland soil, respectively. Soil available P (AP), cation exchange capacity (CEC), and clay content were positively correlated with a and readily desorbable P (RDP), while they were negatively correlated with Q_m ($P < 0.05$); opposite trends were found in the sand content. In addition, the zeta potential of soil colloids decreased with increasing soil pH. Among the cropping systems, the absolute value of zeta potential was lowest for tobacco–walnut intercropping, while its isoelectric point was the highest, resulting in the highest P adsorption capacity.

Conclusions The long-term cropping systems affect P adsorption and desorption characteristics and P availability in red soils by influencing soil physicochemical properties. The main factors driving the changes in P adsorption behavior were AP, CEC, free Fe oxides, and sand content, while AP, sand, and clay contents were the major factors for the P desorption.

Keywords Adsorption–desorption characteristics · Cropping system · Phosphorus · Physicochemical properties · Red soil · Zeta potential

Responsible editor: Zhenli He

Electronic supplementary material The online version of this article (<https://doi.org/10.1007/s11368-019-02493-2>) contains supplementary material, which is available to authorized users.

✉ Yan Cai
caiyya@126.com

¹ College of Resources, Sichuan Agricultural University, Chengdu 611130, China

Abbreviations

P	Phosphorus
MBC	Maximum buffer capacity of soil phosphorus
EPC ₀	Equilibrium phosphorus concentration at zero adsorption
ΔG	Gibbs free energy
RDP	Readily desorbable phosphorus
DPS	Degree of phosphorus saturation
IEP	Isoelectric point

1 Introduction

Phosphorus (P) is a limiting nutrient for agricultural production, and it plays a critical role in ensuring high crop quality and yield (Tilman et al. 2002; Atere et al. 2018). Red soil is widely distributed in regions with abundant rainfall and high temperatures. In particular, red soil is the most prominent soil resource in tropical and subtropical South America, Africa, and Southeast Asia (Li et al. 2017). Due to the strong adsorption of P by iron–aluminum (Fe–Al) oxides, the supply of bioavailable P for crop plants is insufficient in red soil (Foy et al. 1992; Messiga et al. 2011). In the past three decades, to ensure high crop yield, large amounts of chemical P fertilizer have been applied in regions with red soils. This practice directly causes the gradual depletion of phosphate rock resources (Gilbert 2009). In addition, because P fertilizer is easily adsorbed and fixed, approximately 80% of it accumulates in the soil (Withers et al. 2001; Zhu et al. 2018). Subsequent migration of excessive P via rainwater runoff and/or farmland drainage results in eutrophication of water bodies (Hively et al. 2006). Therefore, reducing P adsorption and improving the P use efficiency in red soils is an important area of environmental research.

P adsorption and desorption behaviors are important components of P migration and transformation processes in soils, thus having profound effects on P availability and the environment (Pizzeghello et al. 2011, 2016). P adsorption is a continuous process of adsorption and precipitation. The adsorption process is rapid and reversible, while the precipitation process is slow and irreversible; thus, it is difficult to distinguish the two processes (Arias et al. 2006). As the inverse process of adsorption, P desorption plays a greater role in the availability of soil P and its environmental effects (Heidari et al. 2017; McDonald et al. 2019). Numerous studies have shown that soil Fe–Al oxides, pH, and organic matter (SOM) are the main factors affecting P adsorption and desorption in soils (Boparai and Sharma 2006; Quesada et al. 2011; Fang et al. 2017; Bornø et al. 2018). Fe–Al oxides are the main carriers of variable charge in red soils. Higher pH is associated with a more negative charge on the surface of soil colloids, resulting in the stronger electrostatic rejection of phosphate and reduced P adsorption (Xu et al. 2016; Barrow, 2017). However, the effects of SOM on P adsorption and desorption remain uncertain. Many studies have shown that SOM occupies part of the phosphate adsorption site, resulting in competitive adsorption between P and SOM (Hutchison and Hesterberg 2004; Liu et al. 2018; Zhang et al. 2019). However, a study has suggested that SOM can enhance P adsorption capacity in sandy soils (Debicka et al. 2016).

The effects of cropping systems on soil physical properties (mechanical resistance, particle size composition, and total porosity) and chemical properties (pH and available nutrients) have been well documented (Balota et al. 2014; Viaud et al. 2018). For example, Tran Ba et al. (2016) showed that the

quality of soil was improved (e.g., increased organic carbon concentration) under rice–maize rotation and rice–mung bean rotation compared to under intensive rice continuous cropping. Cheng et al. (2019) found that among cropping systems, SOM content and electrical conductivity were the lowest for corn–wheat rotation, while soil total P concentration was highest for cotton single cropping. Changes in soil properties resulting from the cropping system affect crop growth by regulating the levels of water, gas, heat, and nutrients along with their migration and transformation in the soil; thus, soil properties should be taken into consideration when assessing the effects of cropping systems on P availability (Vinhai-Freitas et al. 2017). Song et al. (2015) found that under different cropping systems, the P adsorption capacity of soils decreased in the following order: paddy soil > rape soil > corn soil > cypress forest soil > wasteland > loquat garden soil in the hilly purple soil areas of southwestern China. Due to intensive weathering and leaching, the response of red soil to cropping systems may differ substantially compared with those of other soils; however, few studies have evaluated the effects of different long-term cropping systems on the P adsorption and desorption characteristics of red soil.

In this paper, we explored the differences in P adsorption and desorption characteristics in red soils under different long-term cropping systems. The specific objectives of this study were (1) to characterize the soil physicochemical properties under different long-term cropping systems; (2) to investigate the soil P adsorption and desorption characteristics within various cropping systems; and (3) to analyze how the cropping systems affect P adsorption–desorption behaviors based on soil physicochemical properties under the experimental conditions. We expect that this study could help design strategies for improving the P availability of the red soil.

2 Materials and methods

2.1 Site description and soil sampling

Soil samples were collected at six locations separated by distances of ~ 1 km in Miyi County, Sichuan Province, China, before sowing in spring 2018. This region has a subtropical climate, with an average annual temperature of 19.7 °C and an average annual rainfall of 1112.6 mm. Farmland soils in this region are mainly red soils based on the China's soil classification system and ultisols according to the US Soil taxonomy (Soil Survey Staff 1999; Zhang et al. 2014). This study focused on red soils whose parent material is viscous alluvium. Six typical cropping systems were selected (one per location): abandoned farmland (control, CK), corn continuous cropping (CC, traditional rotations system), taro continuous cropping (CT), pea–corn rotation (RPC), canola–tobacco rotation (RCT), and walnut–tobacco intercropping (IWT). All these

cropping systems had been converted from traditional rotation systems for more than 10 years along with the social and economic development. The geographical locations and cropping system of each location are listed in Table 1.

Three adjacent plots were selected in each cropping system. The plots were separated by 30 m, and the dimensions of each plot were 20 m × 100 m ($n = 18$). In each plot, six soil cores (diameter = 7.0 cm) were taken from depths of 0–20 cm, avoiding special areas such as fertilization or ridges. Field-moist soil cores from each plot were pooled together to form plot-level composite samples, which were sieved (< 2 mm) to remove any visible rocks, large roots, and coarse plant material. Each soil sample was air-dried and stored at room temperature before analysis.

2.2 Physicochemical analysis

Soil pH was measured in a soil–water (1:2.5, w/v) slurry with a compound electrode (PE-10; Sartorius, Germany). Soil organic matter (SOM) was determined using the potassium dichromate oxidation method with 0.167 M $K_2Cr_2O_7$ (Schollenberger 1931). Total P (TP) was extracted by digestion with HF–HClO₄ and determined via molybdenum–blue colorimetry (Jackson 1958). Available P (AP) was extracted using a solution containing 0.03 M NH_4F and 0.025 M HCl (Bray and Kurtz 1945). Soil texture was analyzed using the hydrometer method (Gee and Bauder 1986). Cation exchange capacity (CEC) was determined by sodium acetate method (US EPA Method 9081). Free Fe–Al oxides were extracted using the sodium dithionite–sodium citrate–bicarbonate (DCB) method, while amorphous Fe–Al oxides were extracted with ammonium oxalate (pH 3.0). Fe and Al in the extracts were determined by inductively coupled plasma–atomic emission spectroscopy (Prodigy 7, Leeman Labs Inc., USA) (Mehra and Jackson 1960).

2.3 Zeta potential measurement

Zeta potential is the potential at the shear plane of the electric double layer on colloidal particles. The value and sign (positive or negative) of the zeta potential depend on the surface charges

of the soil particles. The isoelectric point (IEP) indicates the pH value at which the zeta potential is 0 mV (Xu et al. 2016). The zeta potentials of soil colloids were measured by electrophoresis using a Zetasizer Nano ZS particle size analyzer (ZEN3600, Malvern, Worcestershire, UK). Briefly, 0.05 g of soil sample (0.05 mm) was weighed into a 250-mL Erlenmeyer flask in duplicate followed by the addition of 200 mL of KCl solution (0.01 M). Each suspension was dispersed under ultrasound and then dispensed into four 50-mL plastic bottles (~ 30 mL each). The pH was adjusted to 3, 4, 5, 6, or 7 with HCl or KOH. The zeta potential was measured after 2 h of equilibration (Jiang et al. 2008).

2.4 P adsorption and desorption experiments

The P adsorption and desorption experiments followed the method of Sui and Thompson (2000). In the adsorption experiment, 2.50 g of soil sample was added into a 50-mL centrifugal tube followed by the addition of 25 mL of P working solution (0.01 M $CaCl_2$ with a P concentration of 0, 10, 20, 40, 60, 100, or 150 mg L^{-1}) and three drops of phenol to prevent microbial growth. The mixture was shaken for 24 h (180 rpm at 25 °C) and centrifuged (4000×g) for 10 min. Then, 5 mL of supernatant was transferred into a 25-mL tube, and molybdenum blue spectrophotometry was used to measure the P concentration. In the desorption experiment, the soil samples used in the adsorption experiment were washed twice with saturated NaCl solution and then centrifuged (4000×g for 10 min). After removal of the supernatant, 25 mL of $CaCl_2$ solution (0.01 M) and three drops of phenol were added to each soil sample, followed by shaking for 24 h (180 rpm at 25 °C). After centrifugation (4000×g for 10 min), 5 mL of supernatant was taken to measure the P concentration by molybdenum blue spectrophotometry. The experiments were repeated three times.

2.5 Modeling of P adsorption and desorption

The Langmuir and Freundlich models are most commonly used to quantitatively describe the adsorption characteristics of P on the surfaces of soil particles (Lu et al. 2014). These two adsorption isotherm models are respectively expressed as:

Table 1 General characteristics of the six sampling sites of red soils in Miyi County, Sichuan Province, China

Sample ID	Geographical coordinates	Cropping system	Seasonal gap	Preceding crop	Average P fertilizer application rate (kg ha ⁻¹ year ⁻¹)
CK (Control)	26°48'35" N; 102°09'25" E	Abandoned farmland	Weed	Weed	0
CC	26°48'03" N; 102°09'21" E	Corn continuous cropping	Fallow	Corn	126.7
CT	26°50'12" N; 102°06'42" E	Taro continuous cropping	Fallow	Taro	225.6
RPC	26°47'34" N; 102°09'20" E	Pea–corn rotation	Pea	Corn	686.6
RCT	26°45'28" N; 102°07'25" E	Canola–tobacco rotation	Canola	Tobacco	272.7
IWT	26°48'26" N; 102°08'32" E	Walnut–tobacco intercropping	Walnut	Tobacco	155.8

$$C/Q = C/Q_m + 1/(K \times Q_m), \quad (1)$$

and

$$Q = KC^{1/n}, \quad (2)$$

where C is the P concentration in solution at equilibrium (mg L^{-1}); Q is the P adsorption capacity (mg kg^{-1}); Q_m is the maximum P adsorption capacity (mg kg^{-1}), which is related to the number of phosphate adsorption sites on the surfaces of soil colloids; K (a constant) is the intensity factor of soil P adsorption, with a higher value corresponding to a higher P adsorption intensity (Bache and Williams 1971); and n is a heterogeneity constant related to adsorption intensity.

According to a series of parameters derived from the Langmuir and Freundlich models, the following indices were calculated. The maximum buffer capacity of soil P (MBC, mg kg^{-1}) is a comprehensive parameter that combines P adsorption capacity (Q_m) and intensity (K). It describes the resistance of soil to changes in solution P concentration (Holford 1979). *MBC* is expressed as

$$\text{MBC} = K \times Q_m \quad (3)$$

The equilibrium P concentration at zero adsorption (EPC_0) indicates the ability of the soil to hold P. A smaller EPC_0 value corresponds to a greater ability of the soil to hold P (House and Denison 2000). The formulae for EPC_0 are as follows:

$$\text{Langmuir model : } \text{EPC}_0 = \frac{Q_0}{K(Q_m - Q_0)}, \quad (4)$$

and

$$\text{Freundlich model : } \text{EPC}_0 = \left(\frac{Q_0}{a}\right)^b, \quad (5)$$

where Q_0 is the P concentration in solution when the exogenous P concentration is 0 mg L^{-1} .

The standard Gibbs free energy (ΔG) is an important thermodynamic parameter that indicates the degree of spontaneity of the adsorption process. In this study, the thermodynamic parameters of P adsorption, such as the equilibrium constant (K_c) and ΔG were calculated according to the following Van't Hoff equations (Adhikari and Singh 2003; Huang et al. 2007):

$$K_c = Q/C_e \quad (6)$$

$$\Delta G \text{ (kJ mol}^{-1}\text{)} = -RT \ln K_c \quad (7)$$

where the K_c value calculated in this paper is the average value at different P concentrations; Q and C_e represent the equilibrium concentration of P on soil and in solution (mg L^{-1}), respectively; R is the gas constant ($0.008314 \text{ kJ mol}^{-1} \text{ K}^{-1}$); and T is the absolute temperature in Kelvin.

The degree of P saturation (DPS) indicates the amount of P adsorbed by soil and predicts the P release capacity (Kleinman et al. 2002). The formula of DPS is expressed as:

$$\text{DPS} = \text{AP}/(\text{AP} + Q_m) \times 100\% \quad (8)$$

where AP is the soil available P concentration (mg kg^{-1}) and Q_m is the maximum P adsorption capacity (mg kg^{-1}).

Readily desorbable P (RDP) is the amount of P transferred from the solid phase to the liquid phase in 0.01 M CaCl_2 solution. The P desorption model ($y = ax + b$) was constructed by plotting the amount of desorbed P on the ordinate and the amount of adsorbed P on the abscissa for each soil sample under exogenous P concentrations of 0, 10, 20, 40, 60, 100, and 150 mg L^{-1} using the methods of Lair et al. (2009). In the model, x and y represent the amounts of P adsorption and desorption in soil (mg kg^{-1}), a indicates the concentration of P that can be desorbed on unit P adsorption capacity. A larger a value corresponds to a lower P adsorption capacity and a higher desorption capacity.

2.6 Statistical analysis

All statistical analyses were performed using SPSS 20.0 (IBM SPSS, Somers, NY, USA) and Excel 2013 (Microsoft Corp., Redmond, WA, USA). Data fitting and mapping were conducted using Origin 9.0 (OriginLab Corp., Northampton, MA, USA). Data were subjected to one-way analysis of variance with Tukey's test for pairwise mean comparisons. The relationships between P adsorption–desorption behaviors and soil physicochemical properties were examined by redundancy analysis (RDA) and Pearson's correlation analysis. A P value of less than 0.05 was considered statistically significant.

3 Results

3.1 Soil physicochemical properties under different long-term cropping systems

The physicochemical properties of red soils under the six different cropping systems are listed in Table 2. All soils were acidic or slightly acidic soil conditions. Among all the cropping systems, CC soil had the highest SOM concentration (19.99 g kg^{-1}). RPC soil was a sandy loam, and its sand content was significantly higher (1.56–1.69 times) than those of the other soils (loam clay). RPC soil had the highest TP and AP concentrations (1.01–3.01 and 2.65–11.66 times those in the other soils, respectively). The concentrations of DCB–Fe and DCB–Al were highest in IWT soil (95.72 and 8.28 g kg^{-1} , respectively) and lowest in RPC soil (35.08 and 1.63 g kg^{-1} , respectively). The concentration of Ox–Fe ranged from 2.05 g kg^{-1} (RPC soil) to 3.60 g kg^{-1} (CK soil), while the

Table 2 Basic physicochemical properties of red soils under the six different long-term cropping systems

Soil property	CK	CC	CT	RPC	RCT	IWT
pH	5.18 ± 0.01b	5.26 ± 0.04b	5.29 ± 0.05b	6.78 ± 0.10a	5.46 ± 0.03b	5.36 ± 0.13b
SOM (g kg ⁻¹)	11.74 ± 3.85ab	26.70 ± 5.42a	19.99 ± 6.09ab	9.37 ± 2.94b	12.32 ± 4.35ab	12.57 ± 1.47ab
TP (g kg ⁻¹)	2.13 ± 0.15b	2.32 ± 0.35b	3.98 ± 0.51a	4.03 ± 0.60a	2.24 ± 0.07b	2.70 ± 0.21b
AP (mg kg ⁻¹)	12.54 ± 2.26b	12.82 ± 2.68b	43.96 ± 7.12b	116.64 ± 30.55a	10.07 ± 1.44b	19.55 ± 3.34b
CEC (cmol kg ⁻¹)	7.08 ± 1.19bc	6.32 ± 1.26bc	8.25 ± 0.67b	20.08 ± 4.50a	6.45 ± 1.39bc	3.72 ± 1.25c
DCB-Fe (g kg ⁻¹)	84.25 ± 5.78ab	79.92 ± 2.97b	75.83 ± 5.25b	35.08 ± 4.38c	84.08 ± 4.56ab	95.72 ± 3.18a
DCB-Al (g kg ⁻¹)	5.27 ± 0.28b	5.11 ± 0.20c	5.27 ± 0.49b	1.63 ± 0.49c	6.26 ± 0.40b	8.28 ± 0.32a
Ox-Fe (g kg ⁻¹)	3.60 ± 0.18a	2.81 ± 0.39a	3.25 ± 1.07a	2.05 ± 0.21a	2.20 ± 0.42a	3.20 ± 0.38a
Ox-Al (g kg ⁻¹)	1.19 ± 0.07a	1.45 ± 0.30a	1.60 ± 0.11a	0.52 ± 0.14b	1.24 ± 0.21a	1.48 ± 0.20a
Texture (%)						
Sand	48.5 ± 3.4b	48.7 ± 2.6b	51.3 ± 1.3b	79.8 ± 4.9a	49.7 ± 2.0b	47.1 ± 1.4b
Clay	38.3 ± 1.9a	37.9 ± 2.3a	33.6 ± 1.1a	8.8 ± 1.1b	32.3 ± 1.2a	39.6 ± 1.9a
Silt	13.2 ± 1.7a	13.4 ± 4.9a	15.1 ± 0.3a	11.4 ± 3.9a	18.0 ± 3.2a	13.3 ± 3.3a

Abbreviations of cropping systems are described in Table 1. Data points represent sample means ± standard error ($n = 3$); different lowercase letters in each row represent significant difference among the cropping systems ($P < 0.05$)

SOM soil organic matter, TP total phosphorus, AP available phosphorus, CEC cation exchange capacity, DCB-Fe dithionite extractable Fe oxide, DCB-Al dithionite extractable Al oxide, Ox-Fe oxalate extractable Fe oxide, Ox-Al oxalate extractable Al oxide

concentration of Ox-Al ranged from 0.52 g kg⁻¹ (RPC soil) to 1.60 g kg⁻¹ (CT soil).

3.2 Soil P adsorption characteristics under different long-term cropping systems

The P adsorption capacity of red soils increased with increasing exogenous P concentration, although the increase rate was gradually decreasing (Fig. 1). The differences in P adsorption capacity among the cropping systems became increasingly pronounced with increasing exogenous P concentration. Among cropping system soils, P adsorption capacity at the exogenous P concentration of 150 mg L⁻¹ was highest for CK soil (6.58–223.75% higher than those of the other soils). In general, the P adsorption capacity was highest in CK soil and lowest in RPC soil.

To better understand the P adsorption process in red soils, the adsorption data were fitted by the Langmuir and Freundlich models. The Langmuir model was more suitable for fitting the experimental data in terms of the fitting degree ($R^2 \geq 0.910$). Based on the Langmuir model, the Q_m values of red soils under the different cropping systems ranged from 0.62 to 3.86 g kg⁻¹. The highest value of Q_m was observed in CK soil followed by RCT soil, while RPC soil had the lowest Q_m . The K_L value of RPC soil was 0.033 L mg⁻¹, 1.74–5.50 times those of the other soils. The MBC value ranged from 18.89 L kg⁻¹ (CC soil) to 30.69 L kg⁻¹ (IWT soil). Compared to the EPC₀ value of CK soil, those of RPC and CT soils were 699.42% and 57.35% higher, whereas those of CC, RCT, and IWT soils were 175.40%, 15.28%, and 106.55% lower. Among the cropping systems, the DPS value

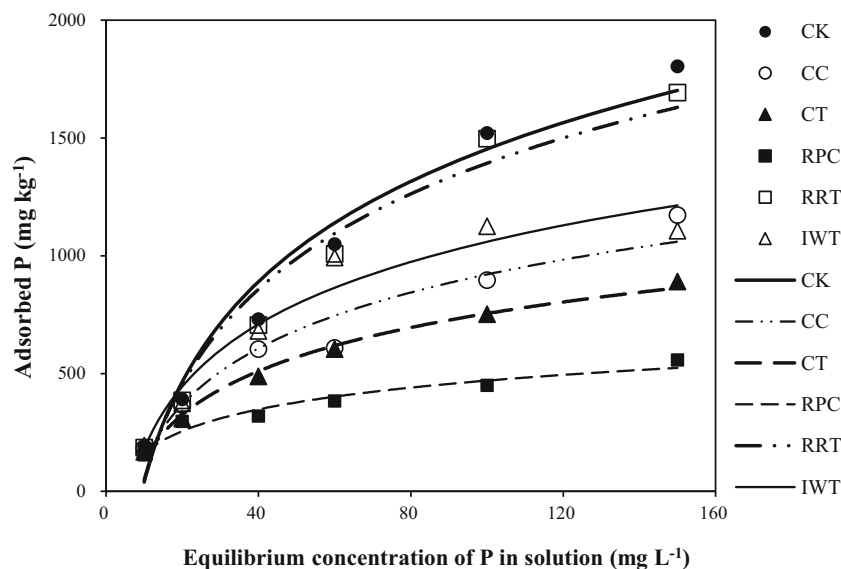
was highest in RPC soil and lowest in RCT soil. Negative ΔG values were observed for all studied soils, indicating the feasibility and spontaneity of the P adsorption (Table 3).

3.3 Soil P desorption characteristics under different long-term cropping systems

The P desorption capacity of red soils under the different cropping systems increased with increasing exogenous P concentration, although the change in the percentage desorbed P had no clear trend (Table S2 – Electronic Supplementary Material - ESM; Fig. 2). The soil P desorption capacity at the same exogenous P concentration considerably differed among the cropping systems. When the exogenous P concentration was 10 or 100 mg L⁻¹, RPC soil had the highest P desorption capacity (49.91 or 107.19 mg kg⁻¹, respectively), while CK soil had the lowest P desorption capacity (6.45 or 32.63 mg kg⁻¹, respectively). When the exogenous P concentration was 150 mg L⁻¹, the P desorption capacity of RPC soil was the highest (122.83 mg kg⁻¹), while that of RCT soil was the lowest (43.82 mg kg⁻¹; 35.68–85.82% lower than those of the other soils; Table S2 - ESM).

To better understand the soil P desorption process, the desorption capacity of soil P was plotted against its adsorption capacity (Fig. 2), and the data were fitted by a linear model (Table S3 - ESM). The a values of the soils under different cropping systems decreased in the following order: RPC > CC > CT = IWT > CK > RCT. Furthermore, most adsorbed P remained in the soil after the desorption experiment, indicating that the adsorption of P was partly irreversible.

Fig. 1 The adsorption isotherms of P in red soils under the six different cropping systems. Abbreviations of cropping systems are defined in Table 1



3.4 Relationship between soil physicochemical properties and P adsorption–desorption behavior

The RDA analysis revealed the contribution of soil physicochemical properties to the adsorption and desorption processes of P in red soils as they were affected by different cropping systems (Fig. 3; Table S4 - ESM). For P adsorption, the first two RDA axes respectively explained 69.49% and 19.21% of the total variation. According to the Monte Carlo permutation test (9999 permutations), soil pH, SOM, TP, AP, CEC, free and amorphous Fe–Al oxides, sand and clay contents were significantly correlated with P adsorption; hence, these environmental factors can be used to explain and predict P adsorption behavior in red soils (Fig. 3). Among these factors, AP ($R^2 = 0.960$), DCB-Fe ($R^2 = 0.896$), sand content ($R^2 = 0.887$), and CEC ($R^2 = 0.866$) had the greatest explanatory power, making them the main environmental drivers of P adsorption. For P desorption, the

first two RDA axes explained 98.41% of the total variation. All the soil physicochemical properties evaluated in this study were significantly correlated with P desorption. Among them, sand content ($R^2 = 0.978$), clay content ($R^2 = 0.937$), AP ($R^2 = 0.937$), and CEC ($R^2 = 0.932$) had the greatest explanatory power (Table S4 - ESM).

According to the Pearson correlations (Table S5 - ESM), Q_m was negatively correlated with soil pH, P concentration (TP and AP), CEC, and sand content, while positive correlation was observed with Fe oxides (DCB-Fe and Ox-Fe), clay content, and silt content ($P < 0.05$). The values of K_L , EPC_0 , DPS, a , and RDP were positively correlated with soil pH, P concentration, CEC, and sand content but negatively correlated with Fe–Al oxides (DCB-Fe, DCB-Al, Ox-Fe, and Ox-Al), clay content, and silt content ($P < 0.01$). Surprisingly, negative correlations were observed between SOM and the P adsorption and desorption parameters, although the correlations were not strong (except MBC and RDP).

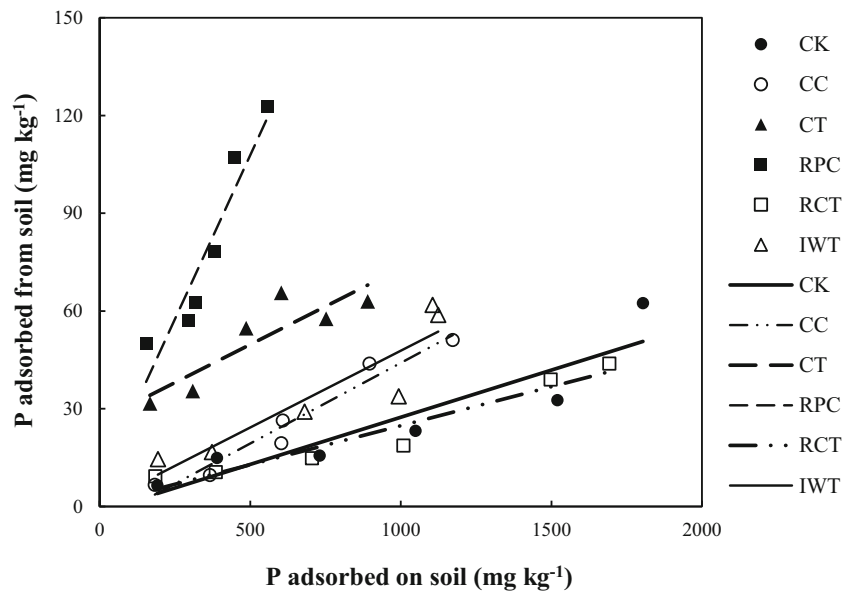
Table 3 Isotherm parameters of the Langmuir and Freundlich models for soil P adsorption

Soil	Langmuir parameters							Freundlich parameters				
	Q_m (mg kg ⁻¹)	K_L (L mg ⁻¹)	R^2	MBC (L kg ⁻¹)	EPC_0 (mg L ⁻¹)	ΔG (kJ mol ⁻¹)	DPS (%)	n	K_F	R^2	EPC_0 (mg L ⁻¹)	
CK	3856.68	0.006	0.995	23.49	0.347	- 6.56	0.33	1.40	53.08	0.979	0.071	
CC	1865.09	0.010	0.959	18.89	0.126	- 3.78	0.69	1.66	57.02	0.975	0.005	
CT	1253.99	0.016	0.999	19.68	0.546	- 1.73	3.51	1.90	66.04	0.980	0.032	
RPC	619.86	0.033	0.910	20.29	2.774	- 0.69	18.82	2.55	76.82	0.947	0.369	
RCT	3477.17	0.007	0.989	23.47	0.301	- 5.53	0.29	1.44	55.15	0.968	0.054	
IWT	1626.27	0.019	0.937	30.69	0.168	- 5.53	1.20	2.03	105.73	0.845	0.002	

Abbreviations of cropping systems are described in Table 1

Q_m the maximum P adsorption capacity, K the P adsorption constant, R^2 the model fitting degree, MBC the maximum buffer capacity of soil P, EPC_0 the equilibrium P concentration at zero adsorption, ΔG the Gibbs free energy, DPS the degree of P saturation

Fig. 2 P desorption isotherms in red soils under the six different cropping systems. Abbreviations of cropping systems are defined in Table 1



The absolute value of zeta potential increased with increasing soil pH and ranked in the following order for the different soils: IWT < CK < CC < RCT < CT < RPC (Fig. 4). This result indicates that the P adsorption capacity of RPC soil was the lowest, while that of

IWT soil was the highest among the cropping systems. The high P adsorption capacity of IWT soil was confirmed by its high IEP, which indicates that the soil surface was positively charged and advantageous to P adsorption.

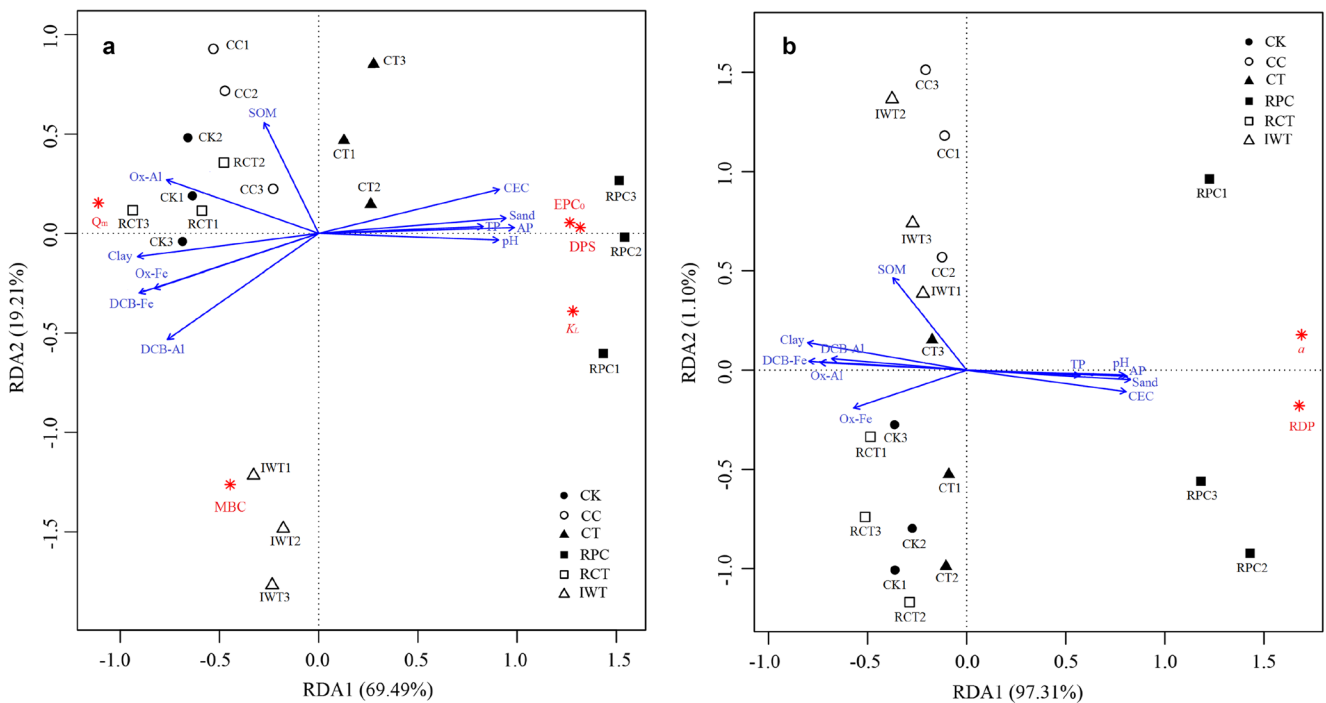


Fig. 3 Ordination plots based on redundancy analysis (RDA) created to explore the relationships between soil P adsorption/desorption and selected soil properties under the six different cropping systems. (a) P adsorption. (b) P desorption. The arrows indicate the lengths and angles between explanatory and response variables and reflect their correlations. Samples

from different long-term cropping systems are marked with different colors and shapes. The numbers following the sample abbreviations indicate the replications. Abbreviations of cropping systems are defined in Table 1. Abbreviations of explanatory and response variables are defined in Tables 2 and 3, respectively

4 Discussion

4.1 Effects of different long-term cropping systems on soil physicochemical properties

Cropping system is an important factor affecting the soil physicochemical properties (Wang et al. 2011; Jiao et al. 2014). First, there are differences in management measures (e.g., fertilization and tillage) and nutrient input across different cropping systems; second, different cropping systems result in varied root morphologies, exudates, and soil microorganisms, which could directly affect the soil physicochemical properties and fertilizer use efficiency (Hartmann et al. 2015; Ai et al. 2018). In the current study, the red soils were acidic or slightly acidic, and the results of zeta potential measurements showed that there was a net negative charge for all the soils (Table 2; Fig. 4). This is probably due to the naturally acidic parent material (granitic) which is characteristic of oxisols. The weathering of the granitic parent material could result in abundant Fe-Al oxides, leading to substantial leaching of soluble soil minerals and basic cations (Tellen and Yerima 2018).

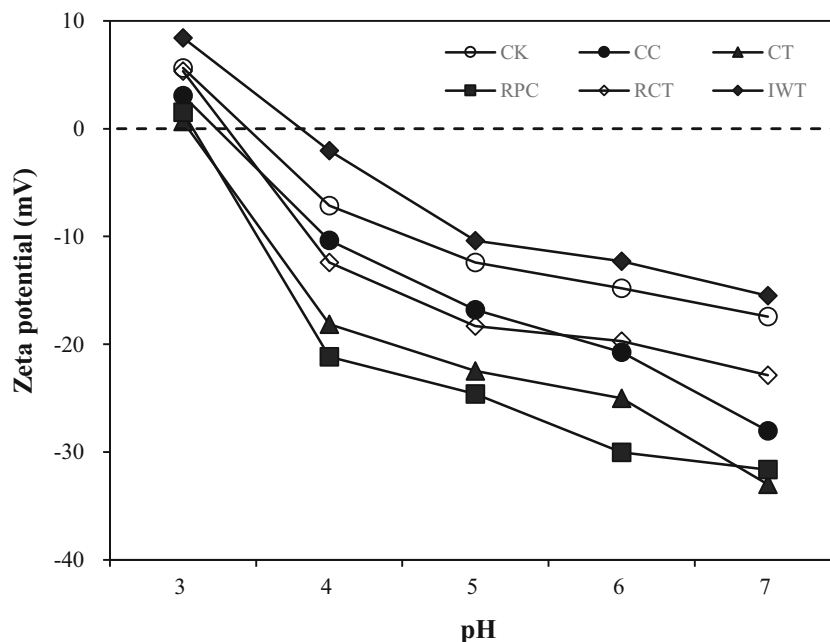
Among the cropping systems studied herein, CC soil resulted in the highest concentration of SOM (Table 2), likely because the biomass of corn straw is high, and organic matter is the main component resulting from the decomposition of crop stubble; thus, most of the carbon is eventually incorporated into the soil (Abiven et al. 2007). The CC field was covered by grasses after corn harvesting, and the huge root biomass of grasses was incorporated into the soil by subsequent plowing. Hence, the CC system could facilitate organic matter inputs into soil for a long term (> 10 years), leading to a positive carbon balance or net increase in SOC stock in the soil profile (Mandal et al. 2012). Moreover, the clay content of CC soil

was high (Table 2), providing physical protection for organic carbon and contributing to the accumulation of organic matter (Six et al., 2000). In addition, among the cropping systems, the AP concentration was highest for RPC soil followed by CT soil (Table 2). First, the high P availability was partly attributed to the high applications of P fertilizer in these soils (Table 1). Second, corn and taro are monocotyledons, and their fibrous root systems could release more organic acids or anions to improve soil P availability by competing for sorption sites with inorganic and organic P, ligand-promoted mineral dissolution (e.g., by affecting the speciation in solution of ions such as Al^{3+}), and stimulating plant growth-promoting microorganisms (e.g., arbuscular mycorrhizal or ectomycorrhizal fungi) (Oburger et al. 2011; Sawers et al. 2017; Lu et al. 2019).

4.2 Effects of different long-term cropping systems on soil P adsorption–desorption behavior

The adsorption and desorption of P in soil can affect P mobility and bioavailability, thus influencing P use efficiency and crop growth (Xiong and Mahmood 2010; Wang and Liang 2014). With increasing exogenous P concentration, the P adsorption capacity of red soils increased, while the differences in P adsorption capacity among the cropping systems became more pronounced (Fig. 1; Table S1 - ESM). This might be related to the differences in the adsorption sites and binding energies of the soils under different cropping systems (Wang et al. 2013). The process of soil P adsorption can be divided into two stages: fast adsorption (chemical) and slow adsorption (physicochemical) (Yang et al. 2019; Lai and Lam 2009). The chemical adsorption dominates the adsorption process at relatively low added P concentrations, and the exchange of ion and ligand is probably the

Fig. 4 Curves of zeta potential vs. pH for red soils under the six different cropping systems. Abbreviations of cropping systems are defined in Table 1



dominant mechanisms contributing to the high P adsorption rate. However, the chemical adsorption process drops rapidly at higher P concentrations, as the available adsorption sites are saturated quickly and the adsorption behavior shifts into physicochemical absorption (Lai and Lam 2009; Wang and Liang 2014). Moreover, numerous studies have found that the P adsorbed by soil cannot be completely desorbed, and most P is retained in the soil. Thus, hysteresis is observed in the kinetics of P adsorption, and the adsorbed P is closely bound to the soil, primarily through bidentate and binucleated bonds (Sander et al. 2005; Guedes et al. 2016; Bai et al., 2018; Bender et al. 2018). In the present study, the a values indicate that the P desorption capacity was highest in RPC soil and lowest in RCT soil (Table S3 - ESM). The low P desorption capacity in the RCT soil was related to its high concentration of amorphous Fe–Al oxides, which resulted in a high activation energy for P adsorption and a high P retention capacity, thereby enhancing the hysteresis effect (Guedes et al. 2016).

The P adsorption and desorption data were fitted by the Langmuir and Freundlich models. Among the cropping systems studied herein, the Q_m was lowest for RPC soil (Table 3), indicating a low P adsorption capacity for this soil. RPC soil had the largest pH, CEC, and absolute value of zeta potential among the studied soils (Table 2; Fig. 4) along with the most negative surface charge and strongest rejection of phosphate anion (Murphy and Stevens 2010; Zhao et al. 2018). The high pH could inhibit the formation of HPO_4^{2-} , which would be first adsorbed by soil colloids (Haynes 1982). Moreover, RPC soil had the lowest concentration of free and amorphous Fe–Al oxides (Table 2). The adsorption of P in acidic soils depends primarily on Fe–Al oxides, especially amorphous Fe–Al oxides (Anderson et al. 1974). Compared to crystalline Fe–Al oxides, amorphous Fe–Al oxides have larger specific surface areas and higher densities of active sites (Ruttenberg and Sulak 2011). In summary, the cropping system affected the soil pH through the root exudation of organic acids and application of physiological acidic fertilizers, etc., which indirectly changed the surface charge and altered the adsorption sites of Fe–Al oxides, thereby influencing P adsorption and desorption.

In the Langmuir model, a K value less than 0.4 L mg^{-1} indicates that P removal from soil solution is attributed to adsorption rather than precipitation (Castro and Torrent 1998). Herein, the K values ranged from 0.007 to 0.033 L mg^{-1} (Table 3), suggesting that P removal occurred via adsorption in all the red soils under different cropping systems. RPC soil had the highest EPC_0 among cropping system soils, indicating that it had the lowest ability to hold P, followed by CT soil. Other studies have found that P leaching occurs in strongly weathered loam clay with DPS exceeding 23%, whereas the threshold DPS value for sandy loam is 14% (Sims et al. 2002; Abdala et al. 2012; Withers et al. 2016). In this study, given the continuous P fertilizer application and low P use efficiency, the soils in which the same cropping system was in place for a long time had high residual P

adsorption capacity and low P saturation. With the exception of the RPC soil, the DPS values of all red soils were far below the threshold value (Table 3). This is because the RPC soil was sandy loam with a low clay content (8.80%; Table 2) but a high proportion of Fe–Al oxides in the clay. The low clay content was not beneficial for the adsorption and fixation of P in RPC soil, resulting in a high risk of P loss from the soil to the environment (Wang et al. 2007).

4.3 Contributions of soil properties to P adsorption and desorption

The effects of soil physicochemical properties on P adsorption–desorption behavior have been discussed previously (Jalali and Jalali 2016; Fang et al. 2017; Liu et al. 2018). Herein, soil clay and silt contents were positively correlated with Q_m and negatively correlated with a in red soils (Table S5 - ESM; $P < 0.01$). The opposite result was observed with sand content in this study, which is consistent with the conclusions of Gérard (2016) and Zhang et al. (2019). This result is attributed to the larger specific surface area and higher CEC of soil clay minerals compared to sand, which facilitated P adsorption (Valladares et al. 2003; Gérard 2016). Furthermore, soil pH, CEC, SOM, Fe–Al oxides, and clay content are reported to be the main physicochemical properties affecting P dynamics in acidic soils (Hartono et al. 2005; Weng et al. 2011; Wang and Liang 2014; Fink et al. 2016). Slightly different conclusions were obtained in the current study. Herein, RDA revealed that the main environmental drivers of P adsorption process in red soils under different long-term cropping systems were AP, CEC, DCB–Fe, and sand content, while AP, sand, and clay contents were the major factors for the P desorption process. In contrast, the effect of SOM on P adsorption was lower than the effects of other soil properties (Table S4), which might be related to organic matter type and soil type (Yang et al. 2019). Notably, SOM was negatively correlated with the P adsorption and desorption parameters (Table S5 - ESM). The possible reasons could be that during P adsorption process, SOM reduced the amount of P adsorbed by competing for adsorption sites and decreasing the binding energy of P adsorption (Fink et al. 2016). During P desorption process, SOM formed smaller and more complex compounds with other ions, thereby blocking channels and preventing the desorption of phosphate adsorbed in the interlayer (Xue et al. 2009).

5 Conclusions

In this study, the long-term cropping systems implemented in red soils altered the characteristics of P adsorption and desorption mainly by affecting soil physicochemical properties. There were considerable differences in soil physicochemical properties among the six cropping systems, especially the

concentrations of P, SOM, Fe–Al oxides, and soil texture, which led to the distinct characteristics of P adsorption and desorption. RPC soil had the lowest P adsorption capacity and highest P desorption capacity among the six cropping systems studied, reflecting in the lowest Q_m value and the highest a value. Furthermore, the main factors driving the changes in P adsorption behavior were AP, CEC, DCB–Fe, and sand content, while AP, sand, and clay contents were the major factors for P desorption in red soils.

Funding information This study was supported by the National Key Research and Development Program of China (No. 2018YFD0200700).

References

- Abdala DB, Ghosh AK, da Silva IR, de Novais RF, Venegas VHA (2012) Phosphorus saturation of a tropical soil and related P leaching caused by poultry litter addition. *Agric Ecosyst Environ* 231:291–295
- Abiven S, Menasseri S, Angers DA, Leterme P (2007) Dynamics of aggregate stability and biological binding agents during decomposition of organic materials. *Eur J Soil Sci* 58:239–247
- Adhikari T, Singh MV (2003) Sorption characteristics of lead and cadmium in some soils of India. *Geoderma* 114:81–92
- Ai C, Zhang SQ, Zhang X, Guo DD, Zhou W, Huang SM (2018) Distinct responses of soil bacterial and fungal communities to changes in fertilization regime and crop rotation. *Geoderma* 319:156–166
- Anderson G, Williams EG, Moir JO (1974) A comparison of the sorption of inorganic phosphate and inositol hexaphosphate by six acid soils. *J Soil Sci* 25:51–62
- Arias M, Silva-Carballal JD, García-Río L (2006) Retention of phosphorus by iron and aluminum-oxides-coated quartz particles. *J Colloid Interface Sci* 295:65–70
- Atere CT, Ge TD, Zhu ZK, Liu SL, Huang XZ, Shbitsova O, Guggenberger G, Wu JS (2018) Assimilate allocation by rice and carbon stabilisation in soil: effect of water management and phosphorus fertilisation. *Plant Soil* 3:1–15
- Bache BW, Williams EG (1971) A phosphate sorption index for soils. *Eur J Soil Sci* 22:289–301
- Bai JH, Ye XF, Jia J, Zhang GL, Zhao QQ, Cui BS, Liu XH (2018) Phosphorus sorption-desorption and effects of temperature, pH and salinity on phosphorus sorption in marsh soils from coastal wetlands with different flooding conditions. *Chemosphere* 188:677–688
- Balota EL, Yada IF, Amaral H, Ankatani AS, Dick RP, Coyne MS (2014) Long-term land-use influences soil microbial biomass P and S, phosphatase and arylsulfatase activities, and S mineralization in a Brazilian Oxisol. *Land Degrad Dev* 25:397–406
- Barrow NJ (2017) The effects of pH on phosphate uptake from the soil. *Plant Soil* 410(1–2):401–410
- Bender MA, Santos DR, Tiecher T, Minella JPG, Barros CAP, Ramon R (2018) Phosphorus dynamics during storm events in a subtropical rural catchment in southern Brazil. *Agric Ecosyst Environ* 261:93–102
- Boparai HK, Sharma KN (2006) Phosphorus adsorption and desorption characteristics of some soils as affected by clay and available phosphorus content. *J Indian Soc Soil Sci* 54(1):111–114
- Bornø ML, Müller-Stöver DS, Liu FL (2018) Contrasting effects of biochar on phosphorus dynamics and bioavailability in different soil types. *Sci Total Environ* 627:963–974
- Bray RH, Kurtz LT (1945) Determination of total, organic and available forms of phosphorus in soil. *Soil Sci* 59:39–46
- Castro B, Torrent J (1998) Phosphate sorption by calcareous Vertisols and Inceptisols as evaluated from extended P-sorption curves. *Eur J Soil Sci* 49(4):661–667
- Cheng ZB, Chen Y, Zhang FH (2019) Effect of cropping systems after abandoned salinized farmland reclamation on soil bacterial communities in arid northwest China. *Soil Tillage Res* 187:204–213
- Debicka M, Kocowicz A, Weber J, Jamroz E (2016) Organic matter effects on phosphorus sorption in sandy soils. *Arch Agron Soil Sci* 62:840–855
- Fang HW, Cui ZH, He GJ, Huang L, Chen MH (2017) Phosphorus adsorption onto clay minerals and iron oxide with consideration of heterogeneous particle morphology. *Sci Total Environ* 605–606:357–367
- Fink JR, Inda AV, Bavaresco J, Barrón V, Torrent J, Bayer C (2016) Adsorption and desorption of phosphorus in subtropical soils as affected by management system and mineralogy. *Soil Tillage Res* 155:62–68
- Foy CD, Duke JA, Devine TE (1992) Tolerance of soybean germplasm to an acid Tatum subsoil. *J Plant Nutr* 15:527–547
- Gee GW, Bauder JW (1986) Particle fraction and particle size analysis. In: Klute A (ed) *Methods of soil analysis, part 1*, 2nd edn. ASA and SSSA, Madison
- Gérard F (2016) Clay minerals, iron/aluminum oxides, and their contribution to phosphate sorption in soils—a myth revisited. *Geoderma* 262:213–226
- Gilbert N (2009) Environment: the disappearing nutrient. *Nature* 461:716–718
- Guedes RS, Melo LCA, Vergütz L, Rodríguez-Vila A, Covelo EF, Fernandes AR (2016) Adsorption and desorption kinetics and phosphorus hysteresis in highly weathered soil by stirred flow chamber experiments. *Soil Tillage Res* 162:46–54
- Hartmann M, Frey B, Mayer J, Mäder P, Widmer F (2015) Distinct soil microbial diversity under long-term organic and conventional farming. *ISME J* 9:1177–1194
- Hartono A, Funakawa S, Kosaki T (2005) Phosphorus sorption-desorption characteristics of selected acid upland soils in Indonesia. *Soil Sci Plant Nutr* 51:787–799
- Haynes RJ (1982) Effects of liming on phosphate availability in acid soils. *Plant Soil* 68:289–308
- Heidari S, Reyhanitabar A, Oustan S (2017) Kinetics of phosphorus desorption from calcareous soils using DGT technique. *Geoderma* 305:275–280
- Hively WD, Gerard-Marchant P, Steenhuis TS (2006) Distributed hydrological modeling of total dissolved phosphorus transport in an agricultural landscape. II. Dissolved phosphorus transport. *Hydrol Earth Syst Sci* 10:263–276
- Holford ICR (1979) Evaluation of soil phosphate buffering indices. *Soil Res* 17:495–504
- House WA, Denison FH (2000) Factors influencing the measurement of equilibrium phosphate concentrations in river sediments. *Water Res* 34(4):1187–1200
- Huang X, Gao NY, Zhang QL (2007) Thermodynamics and kinetics of cadmium adsorption onto oxidized granular activated carbon. *J Environ Sci* 19:1287–1292
- Hutchison KJ, Hesterberg D (2004) Dissolution of phosphate in a phosphorus enriched Ultisol as affected by microbial reduction. *J Environ Qual* 33:1793–1802
- Jackson ML (1958) *Soil chemical analysis*. Soil Chem Anal. Englewood Cliffs, New Jersey, USA: Prentice-Hall
- Jalali M, Jalali M (2016) Relation between various soil phosphorus extraction methods and sorption parameters in calcareous soils with different texture. *Sci Total Environ* 566–567:1080–1093
- Jiang J, Xu RK, Wang Y, Zhao AZ (2008) The mechanism of chromate sorption by three variable charge soils. *Chemosphere* 71:1469–1475

- Jiao SY, Zhang M, Wang YM, Liu JQ, Li YQ (2014) Variation of soil nutrients and particle size under different vegetation types in the Yellow River Delta. *Acta Ecol Sin* 34:148–153
- Kleinman PJA, Sharpley AN, Moyer BG, Elwinger GF (2002) Effect of mineral and manure phosphorus sources on runoff phosphorus. *J Environ Qual* 31:2026–2033
- Lai DYF, Lam KC (2009) Phosphorus sorption by sediments in a subtropical constructed wetland receiving stormwater runoff. *Ecol Eng* 35:735–743
- Lair GJ, Zehetner F, Khan ZH, Gerzabek MH (2009) Phosphorus sorption-desorption in alluvial soils of a young weathering sequence at the Danube River. *Geoderma* 149:39–44
- Li QX, Jin ZW, Chen XM, Jing Y, Huang QR, Zhang JB (2017) Effects of biochar on aggregate characteristics of upland red soil in subtropical China. *Environ Earth Sci* 76:372
- Liu Y, Zhu ZQ, He XS, Yan C, Du YQ, Huang YD, Su P, Wang S, Zheng XX, Xue YJ (2018) Mechanisms of rice straw biochar effects on phosphorus sorption characteristics of acid upland red soils. *Chemosphere* 207:267–277
- Lu HY, Yang LZ, Shabbir S (2014) The adsorption process during inorganic phosphorus removal by cultured periphyton. *Environ Sci Pollut Res* 21(14):8782–8791
- Lu JY, Dijkstra FA, Wang P, Cheng WX (2019) Roots of non-woody perennials accelerated long-term soil organic matter decomposition through biological and physical mechanisms. *Soil Biol Biochem* 134:42–53
- Mandal KG, Baral U, Padhi J, Majhi P, Chakraborty H, Kumar A (2012) Effects of cropping on soil properties and organic carbon stock in Deras region, India. *Reg Environ Chang* 12(4):899–912
- McDonald GJ, Norton SA, Fernandez JJ, Hoppe KM, Dennis J, Amirbahman A (2019) Chemical controls on dissolved phosphorus mobilization in a calcareous agricultural stream during base flow. *Sci Total Environ* 660:876–885
- Mehra OP, Jackson ML (1960) Iron oxide removal from soils and clays by a dithionite-citrate system buffered with sodium bicarbonate. In: Swineford ADA (ed) *National Conference on Clays and Clay Minerals*. Washington
- Messiga AJ, Ziadi N, Angers DA, Morel C, Parent LE (2011) Tillage practices of a clay loam soil affect soil aggregation and associated C and P concentrations. *Geoderma* 164:225–231
- Murphy PNC, Stevens RJ (2010) Lime and gypsum as source measures to decrease phosphorus loss from soils to water. *Water Air Soil Pollut* 212:101–111
- Oburger E, Jones DL, Wenzel WW (2011) Phosphorus saturation and pH differentially regulate the efficiency of organic acid anion-mediated P solubilization mechanisms in soil. *Plant Soil* 341:363–382
- Pizzeghello D, Berti A, Nardi S, Morari F (2011) Phosphorus forms and P sorption properties in three alkaline soils after long-term mineral and manure applications in northeastern Italy. *Agric Ecosyst Environ* 141(1):58–66
- Pizzeghello D, Berti A, Nardi S, Morari F (2016) Relationship between soil test phosphorus and phosphorus release to solution in three soils after long-term mineral and manure application. *Agric Ecosyst Environ* 233:214–223
- Quesada CA, Lloyd J, Anderson LO, Fyllas NM, Schwarz M, Czimczik CI (2011) Soil of Amazonia with particular reference to the rainforest sites. *Biogeosciences* 8(6):3851–3921
- Ruttenberg KC, Sulak DJ (2011) Sorption and desorption of dissolved organic phosphorus onto iron (oxyhydr) oxides in seawater. *Geochim Cosmochim Acta* 75:4095–4112
- Sander M, Lu Y, Pignatello JJ (2005) A thermodynamically based method to quantify true sorption hysteresis. *J Environ Qual* 34:1063–1072
- Sawers RJ, Svane SF, Quan C, Gronlund M, Wozniak B, Gebreselassie MN, Gonzalez-Munoz E, Chavez Montes RA, Baxter I, Goudet J, Jakobsen I, Paszkowski U (2017) Phosphorus acquisition efficiency in arbuscular mycorrhizal maize is correlated with the abundance of root-external hyphae and the accumulation of transcripts encoding *PHT1* phosphate transporters. *New Phytol* 214:632–643
- Schollenberger CJ (1931) Determination of soil organic matter. *Soil Sci* 31:483–486
- Sims JT, Maguire RO, Leytem AB, Gartley KL, Pautler MC (2002) Evaluation of Mehlich-3 as an agri-environmental soil phosphorus test for the mid-Atlantic United States of America. *Soil Sci Soc Am J* 66:2016–2032
- Six J, Paustian K, Elliott ET, Combrink C (2000) Soil structure and soil organic matter. I. Distribution of aggregate size classes and aggregate associated carbon. *Soil Sci Soc Am J* 64:681–689
- Soil Survey Staff (1999) *Soil taxonomy: a basic system of soil classification for making and interpreting soil surveys*. USDA Soil Conservation Service, Washington
- Song C, Xu M, Zhao W, Xu F, Zhang T, Yang WY (2015) Study on phosphorus availability and its related affecting factors of purple soil under different types of land use. *J Soil Water Conserv (China)* 29(06):85–89+95
- Sui YB, Thompson ML (2000) Phosphorus sorption, desorption, and buffering capacity in a biosolids-amended Mollisol. *Soil Sci Soc Am J* 64(1):164–169
- Tellen VA, Yerima BPK (2018) Effects of land use change on soil physicochemical properties in selected areas in the North West region of Cameroon. *Environ Syst Res* 7:3
- Tilman D, Cassman KG, Matson PA, Naylor R, Polasky S (2002) *Agricultural sustainability and intensive production practices*. *Nature* 418:671–677
- Tran Ba L, Le Van K, Van Elsacker S, Cornelis WM (2016) Effect of cropping system on physical properties of clay soil under intensive rice cultivation. *Land Degrad Dev* 27(4):973–982
- Valladares GS, Pereira MG, Dos Anjos LHC (2003) Phosphate sorption in low activity clay soil. *Bragantia* 62(1):111–118
- Viaud V, Santillán-Carvantes P, Akkal-Corfini N, Le Guillou C, Prévost-Bouré NC, Ranjard L, Menasseri-Aubry S (2018) Landscape-scale analysis of cropping system effects on soil quality in a context of crop-livestock farming. *Agric Ecosyst Environ* 265:166–177
- Vinhal-Freitas IC, Corrêa's GF, Wendling B, Bobul'ská L, Ferreira AS (2017) Soil textural class plays a major role in evaluating the effects of land use on soil quality indicators. *Ecol Indic* 74:182–190
- Wang LQ, Liang T (2014) Effects of exogenous rare earth elements on phosphorus adsorption and desorption in different types of soils. *Chemosphere* 103:148–155
- Wang DR, Jin XC, Zhao HC, Zhou XN, Wu FC (2007) Effects of hydrilla *Verticillata* on phosphorus retention and release in sediments. *Water Air Soil Pollut* 181(1–4):329–339
- Wang LY, Han YZ, Zhang CL, Pei ZY (2011) Reclaimed soil properties and weathered gangue change characteristics under various vegetation types on gangue pile. *Acta Ecol Sin* 31(21):6429–6441
- Wang XY, Zhang LP, Zhang FF, Zhang HS, Mei D (2013) Phosphorus adsorption by soils from four land use patterns. *Asian J Chem* 25(1):282–286
- Weng LP, Vega FA, van Riemsdijk WH (2011) Competitive and synergistic effects in pH dependent phosphate adsorption in soils: LCD modeling. *Environ Sci Technol* 45:8420–8428
- Withers PJA, Edwards AC, Foy RH (2001) Phosphorus cycling in UK agriculture and implications for phosphorus loss from soil. *Soil Use Manag* 17:139–149
- Withers PJA, Flynn NJ, Warren GP, Taylor M, Chambers BJ (2016) Sustainable management of biosolid phosphorus: a field study. *Soil Use Manag* 32(S1):54–63
- Xiong JB, Mahmood Q (2010) Adsorptive removal of phosphate from aqueous media by peat. *Desalination* 259(1):59–64
- Xu RK, Qafoku NP, Van Ranst E, Li JY, Jiang J (2016) Adsorption properties of subtropical and tropical variable charge soils:

- implications from climate change and biochar amendment. *Adv Agron* 135:1–58
- Xue YJ, Hou HB, Zhu SJ (2009) Characteristics and mechanisms of phosphate adsorption onto basic oxygen furnace slag. *J Hazard Mater* 162:973–980
- Yang XY, Chen XW, Yang XT (2019) Effect of organic matter on phosphorus adsorption and desorption in a black soil from Northeast China. *Soil Tillage Res* 187:85–91
- Zhang WL, Xu AG, Zhang RL, Ji HJ (2014) Review of soil classification and revision of China soil classification system. *J Integr Agr (China)* 47:3214–3230
- Zhang YH, Huang SM, Guo DD, Zhang SQ, Song X, Yue K, Zhang KK, Bao DJ (2019) Phosphorus adsorption and desorption characteristics of different textural fluvo-aquic soils under long-term fertilization. *J Soils Sediments* 19(3):1306–1318
- Zhao ZJ, Jin R, Fang D, Wang H, Dong Y, Xu RK, Jiang J (2018) Paddy cultivation significantly alters the forms and contents of Fe oxides in an Oxisol and increases phosphate mobility. *Soil Tillage Res* 184: 176–180
- Zhu J, Li M, Whelan M (2018) Phosphorus activators contribute to legacy phosphorus availability in agricultural soils: a review. *Sci Total Environ* 612:522–537

Publisher's note Springer Nature remains neutral with regard to jurisdictional claims in published maps and institutional affiliations.